

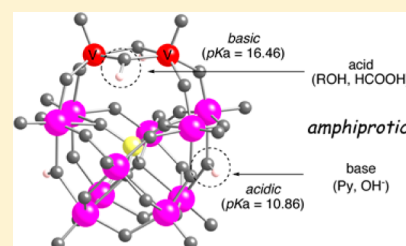
# Amphiprotic Properties of a Bis( $\mu$ -hydroxo)divanadium(IV)-Substituted $\gamma$ -Keggin-Type Silicodecatungstate Containing Two Different Kinds of Hydroxyl Moieties

Kazuhiro Uehara, Takuya Miyachi, and Noritaka Mizuno\*

Department of Applied Chemistry, School of Engineering, The University of Tokyo, 7-3-1 Hongo, Bunkyo-ku, Tokyo 113-8656, Japan

## S Supporting Information

**ABSTRACT:** A bis( $\mu$ -hydroxo)divanadium(IV)-substituted  $\gamma$ -Keggin-type silicodecatungstate,  $(\text{TBA})_4[\gamma\text{-SiV}^{\text{IV}}_2\text{W}_{10}\text{O}_{36}(\mu\text{-OH})_4]$  (**1**), possesses two different kinds of hydroxyl groups and can work as an amphiprotic species to accept and donate proton(s). Dehydrative condensation reactions of **1** with methanol and formic acid proceed on more basic hydroxyl groups between two vanadium atoms without the deprotonation of more acidic hydroxides between two tungsten atoms to form  $(\text{TBA})_4[\gamma\text{-SiV}^{\text{IV}}_2\text{W}_{10}\text{O}_{36}(\mu\text{-OH})_3(\mu\text{-OR})]$  (**2**·**R**, **R** = Me, Et, Pr; **3**, **R** = C(O)H), showing Brønsted base properties of the hydroxyl groups between two vanadium atoms. On the other hand, the hydroxyl groups between tungsten atoms exhibit Brønsted acid properties and react with pyridine (Py) and TBAOH to form  $(\text{TBA})_4\text{X}[\gamma\text{-SiV}^{\text{IV}}_2\text{W}_{10}\text{O}_{37}(\mu\text{-OH})_3]$  (**PyH**·**4**, **X** = PyH; **TBA**·**4**, **X** = TBA). DFT calculations for  $[\gamma\text{-SiV}^{\text{IV}}_2\text{W}_{10}\text{O}_{36}(\mu\text{-OH})_4]^{4-}$  in water also support both the acidic and basic nature of hydroxyl groups in **1**.



## INTRODUCTION

In 1923, the Brønsted–Lowry theory disclosed the definition of a Brønsted acid and base: the Brønsted acid possesses the ability to donate a proton ( $\text{H}^+$ ), whereas the Brønsted base does the ability to accept a proton.<sup>1</sup> Generally, s-block metal (alkali and alkaline earth metals) hydroxides work as Brønsted bases, whereas p-block metal hydroxides work as Brønsted acids.<sup>2</sup> The differences in the acid–base properties are generally derived from the characters of metal–oxygen bonds (i.e., ionic vs covalent). Since these properties for the transition-metal hydroxides are also dependent upon the oxidation states of the metal centers, studies on the acid–base properties of transition-metal hydroxo complexes are more complicated and have become important subjects of modern chemistry. In contrast, polybasic acids with more than two protons sometimes act as amphiprotic species and react with both acidic and basic molecules.<sup>3</sup> These molecules *stepwise* release protons and neutralize basic molecules *stepwise* to form corresponding conjugate bases. Since *inorganic* polybasic acids generally consist of symmetric hydroxides such as  $\text{H}_2\text{O}$ ,  $\text{H}_2\text{SO}_4$ , and  $\text{H}_3\text{PO}_4$ , polybasic acids with different kinds of hydroxyl groups (dissymmetric hydroxyl groups) are still rare, whereas there are several dissymmetric organic polyacids such as hydroxybenzoic acids and amino acids.<sup>4</sup> The more basic hydroxide groups never react *prior* to the more acidic ones, and the coexistence of both acid and basic hydroxide groups inside the same molecules are considered to be difficult.

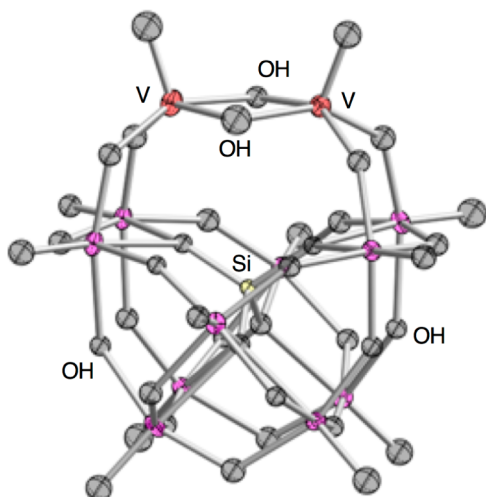
Polyoxometalates (POMs) are recognized as inorganic polybasic acids and have been utilized as acid and oxidation catalysts, pharmaceuticals, building blocks of inorganic–organic hybrid materials, and so forth.<sup>5</sup> While a recent advance of X-ray

crystallography enables us to determine various molecular structures of POM derivatives, little is known about those interacting with the organic molecules.<sup>6,7</sup> Very recently, we have successfully synthesized a bis( $\mu$ -hydroxo)divanadium(IV)-substituted  $\gamma$ -Keggin-type POM,  $(\text{TBA})_4[\gamma\text{-SiV}^{\text{IV}}_2\text{W}_{10}\text{O}_{36}(\mu\text{-OH})_4]$  (**1**; TBA = tetra-*n*-butylammonium), with two kinds of V–OH–V and W–OH–W hydroxides (Chart 1).<sup>7a</sup> The hydroxyl groups between two tungsten atoms in **1** exhibit acidic properties and react with phenyl isocyanate to form  $(\text{TBA})_4[\gamma\text{-SiV}^{\text{IV}}_2\text{W}_{10}\text{O}_{38}(\mu\text{-OH})_2(\text{PhNHCO})_2]$ , containing N-protonated phenyl isocyanate species. In contrast, the hydroxyl groups between two vanadium atoms in the bis( $\mu$ -hydroxo)-divanadium(V)-substituted POM  $(\text{TBA})_4[\gamma\text{-SiV}^{\text{V}}_2\text{W}_{10}\text{O}_{36}(\mu\text{-OH})_2]$  (**A**) exhibit basic properties and react with alcohols to form the ( $\mu$ -alkoxo)divanadium(V)-substituted derivatives  $(\text{TBA})_4[\gamma\text{-SiV}^{\text{V}}_2\text{W}_{10}\text{O}_{36}(\mu\text{-OH})(\mu\text{-OR})]$ .<sup>7b,c</sup> Although a similar basic reactivity of the bis( $\mu$ -hydroxo)divanadium(IV) core in **1** is expected, the reactivity has never been investigated. Therefore, we came up with the idea that compound **1** acts as an amphiprotic species containing acidic and basic hydroxides. Herein, we investigate the unusual amphiprotic properties of **1** with density functional theory (DFT) calculations and its reactivities toward several substrates such as pyridine, TBAOH, alcohols, and formic acid.

Received: March 20, 2014

Published: May 7, 2014

**Chart 1. Molecular Structure of  $(\text{TBA})_4[\gamma\text{-SiV}^{\text{VI}}_2\text{W}_{10}\text{O}_{38}(\mu\text{-OH})_4]$  (1) Drawn at the 50% Probability Level<sup>a</sup>**



<sup>a</sup>TBAs are omitted for clarity.

## RESULTS AND DISCUSSION

**Electron Configurations of  $(\text{TBA})_4[\gamma\text{-SiV}^{\text{IV}}_2\text{W}_{10}\text{O}_{36}(\mu\text{-OH})_4]$  (1).** DFT calculations for the anionic moieties of  $(\text{TBA})_4[\gamma\text{-SiV}^{\text{IV}}_2\text{W}_{10}\text{O}_{36}(\mu\text{-OH})_4]$  in acetonitrile were carried out using the 6-31G\* (O, Si, H)/LanL2DZ (V, W) hybrid basis set with the UB3LYP level of theory with the conductor-like polarizable continuum model (IEFPCM).<sup>8–10</sup> Since the

calculated results reproduced well those of X-ray crystallography, the electron configurations of **1** could be elucidated properly. Compound **1** possessed the triplet ( $S = 1$ ) spin state, each electron singly occupied  $\alpha 254$  (SOMO1) and  $\alpha 255$  (SOMO2) orbitals with energies of  $-6.121$  and  $-4.418$  eV, respectively (Figure 1). SOMO1 was mainly concerned with the V(101) (coefficient of  $d_{x^2-y^2}$  orbital = 0.66842), whereas SOMO2 was mainly concerned with W(109)–W(112) (the respective coefficients of  $d_{xy}$  orbitals are 0.44698, 0.21122, 0.16835, and 0.28912), showing that two electrons are not localized on the vanadium atoms but are delocalized throughout the anionic part of **1**. The V<sup>IV</sup>...O(–Si) distances (calcd, 2.956 and 3.024 Å; found by X-ray, 2.90(1) and 2.91(1) Å) were longer than those of the vanadium(V) derivative  $(\text{TBA})_4[\gamma\text{-SiV}^{\text{V}}_2\text{W}_{10}\text{O}_{38}(\mu\text{-OH})_2]$  (**A**; calcd, 2.616 and 2.618 Å; found by X-ray, 2.51(2) and 2.53(1) Å) due to the Jahn–Teller effect characteristic of  $d^1$  transition-metal complexes. As a result, the  $p_z$  orbitals of the  $\text{SiO}_4$  unit in **1** were destabilized and became HOMOs with energies of  $-7.272$  and  $-7.263$  eV, respectively (i.e., coefficients of  $p_z$  orbitals of O137 and O138 in  $\alpha 253$  were  $-0.23711$  and  $0.31068$ , respectively, and those in  $\beta 253$  were  $-0.22571$  and  $0.29790$ , respectively), whereas the  $p_z$  orbital of the  $\text{SiO}_4$  unit in **A** was observed at HOMO-1.

In order to determine the deprotonation pathway from **1**, DFT calculations for the anionic moieties of the deprotonated species in water were carried out at the same level of theory, and the corresponding single-point energies in water were calculated with the 6-311++G\*\* (O, H)/6-31G\* (Si)/LanL2DZ (V, W) hybrid basis set with the B3LYP level of

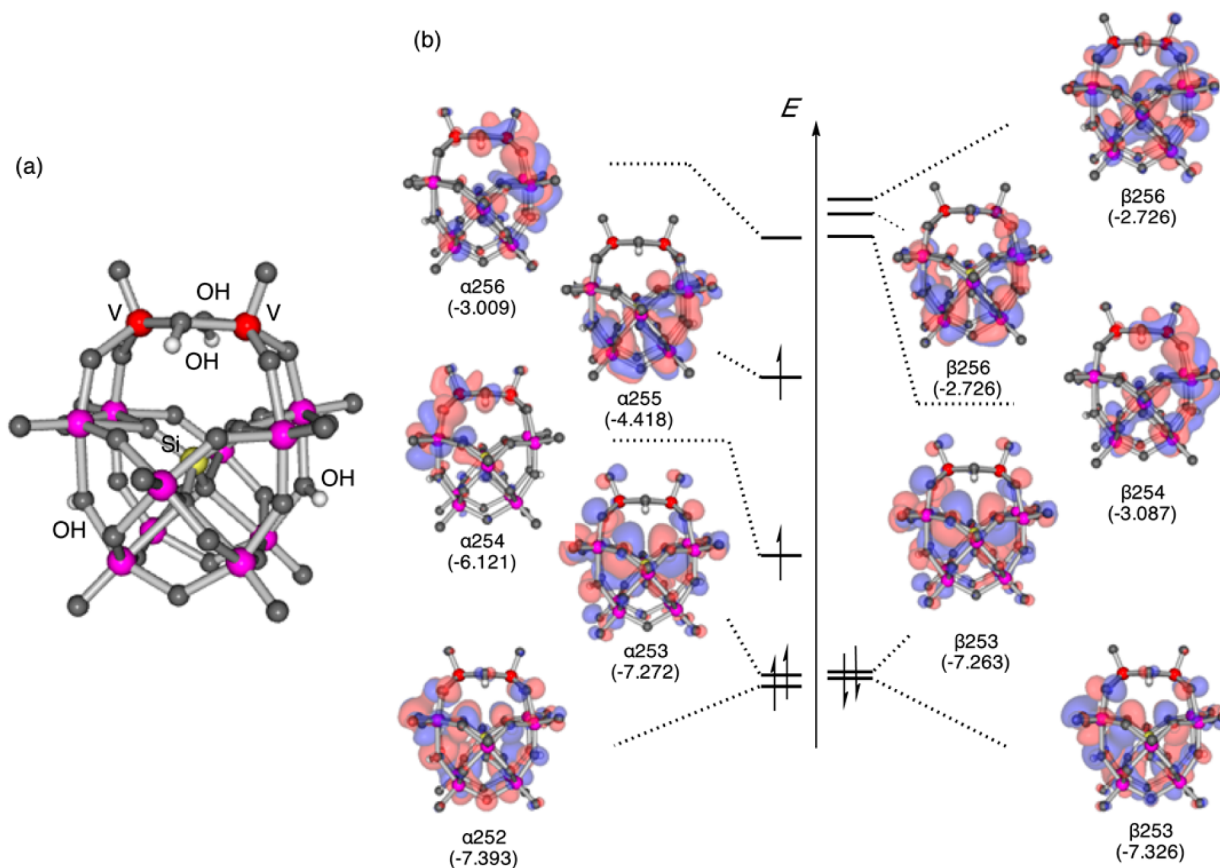


**Figure 1.** (a) Optimized structure and (b) energy diagram (isosurface value 0.100) of  $[\gamma\text{-SiV}^{\text{IV}}_2\text{W}_{10}\text{O}_{36}(\mu\text{-OH})_4]^{4-}$  (**1**) with DFT calculations. Energies in parentheses are in eV.

theory (Table 1 and Table S9 (Supporting Information)). There are six possible deprotonation pathways for (W-)O-H

**Table 1.**  $\Delta G^\circ$  and  $pK_a$  Values of the Deprotonations of  $(TBA)_4[\gamma-SiV_2W_{10}O_{36}(\mu-OH)_4]$  (**1**) with DFT Calculations

reaction <sup>a</sup>	$\Delta G^{ob,c}$	$pK_a$
$1_{aq} \rightarrow a_{aq} + H_3O^+$ (step 1 $\rightarrow$ a)	63.22	11.32
$1_{aq} \rightarrow a'_{aq} + H_3O^+$ (step 1 $\rightarrow$ a')	94.16	16.86
$a_{aq} \rightarrow b_{aq} + H_3O^+$ (step a $\rightarrow$ b)	99.30	17.78
$a_{aq} \rightarrow b''_{aq} + H_3O^+$ (step a $\rightarrow$ b'')	127.92	22.42
$b_{aq} \rightarrow c_{aq} + H_3O^+$ (step b $\rightarrow$ c)	141.96	25.42
$c_{aq} \rightarrow d_{aq} + H_3O^+$ (step c $\rightarrow$ d)	208.90	37.41

<sup>a</sup>H<sub>2</sub>O was evaluated as the conductor-like polarizable model (IEFPCM) considering the relative permittivity. <sup>b</sup> $\Delta G^{solv}(H_3O^+) = -1112.52 \text{ kJ mol}^{-1}$  ( $-265.9 \text{ kcal mol}^{-1}$ ) cited from ref 11 was taken into account. <sup>c</sup>Energy in  $\text{kJ mol}^{-1}$ .

and (V-)O-H moieties in **1** (Figure S7 (Supporting Information)), and the main deprotonation pathway is depicted in Figure 2. At the first deprotonation, the  $\Delta G^\circ$  values of the steps **1**  $\rightarrow$  a and **1**  $\rightarrow$  a' were 63.22 and 94.16  $\text{kJ mol}^{-1}$ , respectively, showing that the deprotonation proceeds at the hydroxide between two tungsten atoms. Successively, at the second deprotonation, the  $\Delta G^\circ$  values of the steps a  $\rightarrow$  b and a  $\rightarrow$  b'' were 99.30 and 127.92  $\text{kJ mol}^{-1}$ , respectively, also showing that the deprotonation proceeds at the hydroxide between two tungsten atoms. Finally, the deprotonations proceed from two hydroxides between two vanadium atoms. The deprotonation from the (W-)O-H moieties proceeds prior to the deprotonation from (V-)O-H moieties. As a result, the most probable deprotonations proceed in the order **1**

$\rightarrow$  a  $\rightarrow$  b  $\rightarrow$  c  $\rightarrow$  d, and the  $pK_a$  values of the steps **1**  $\rightarrow$  a, a  $\rightarrow$  b, b  $\rightarrow$  c, and c  $\rightarrow$  d are 11.32, 17.78, 25.42, and 37.41, respectively.

**Basic Property of  $(TBA)_4[\gamma-SiV_2W_{10}O_{36}(\mu-OH)_4]$  (**1**).** Reactions of **1** with excess alcohols and formic acid as Brønsted acids gave the corresponding alkoxy and formate derivatives  $(TBA)_4[\gamma-SiV_2W_{10}O_{36}(\mu-OH)_3(\mu-OR)]$  (**2**·R, R = Me (55%), R = Et (63%), R = Pr (82%); **3** (61%), R = C(O)H) and the dehydrative condensation reactions proceeded at the divanadium core (Figure 1c,d).<sup>7b-e</sup> CSI-MS measurements for **2**·R (R = Me, Et, *n*-Pr) and **3** (R = C(O)H) showed signals at *m/z* 3839.22 (3838.63, TBA·**2**·Me<sup>+</sup>), 3852.14 (3852.74, TBA·**2**·Et<sup>+</sup>), 3866.30 (3866.67, TBA·**2**·Pr<sup>+</sup>), and 3852.59 (3852.62, TBA·**3**<sup>+</sup>), respectively, indicating the formations of the corresponding monosubstituted derivatives (Figures S15–S18 (Supporting Information)).

Molecular structures of all compounds were successfully determined by X-ray crystallography (Figure 3a,b, Figures S1–S4 (Supporting Information), Tables 2 and 3, and Tables S1 and S2 (Supporting Information)). The methoxy and formate bridging ligands were disordered and observed at both sides of bridging oxygen sites between two vanadium atoms with an occupancy of ca. 0.5.<sup>12,13</sup> Therefore, one of two bridging oxygen atoms between two vanadium atoms is assignable as a hydroxide. The bond valence sum (BVS) values for O(114), O(125), and O(127) of **2**·Me were 1.296, 1.520, and 1.145, respectively, and those of **3** were 1.157, 1.611, and 1.667, respectively, suggesting that these valences in **2**·Me and **3** are  $-1$  (Tables S5 and S8 (Supporting Information)).<sup>14</sup> The BVS values for V (4.454, 4.351), W (5.865–6.313), O (1.644–2.055), and Si (4.065) of **2**·Me and those for V (4.172, 4.303),

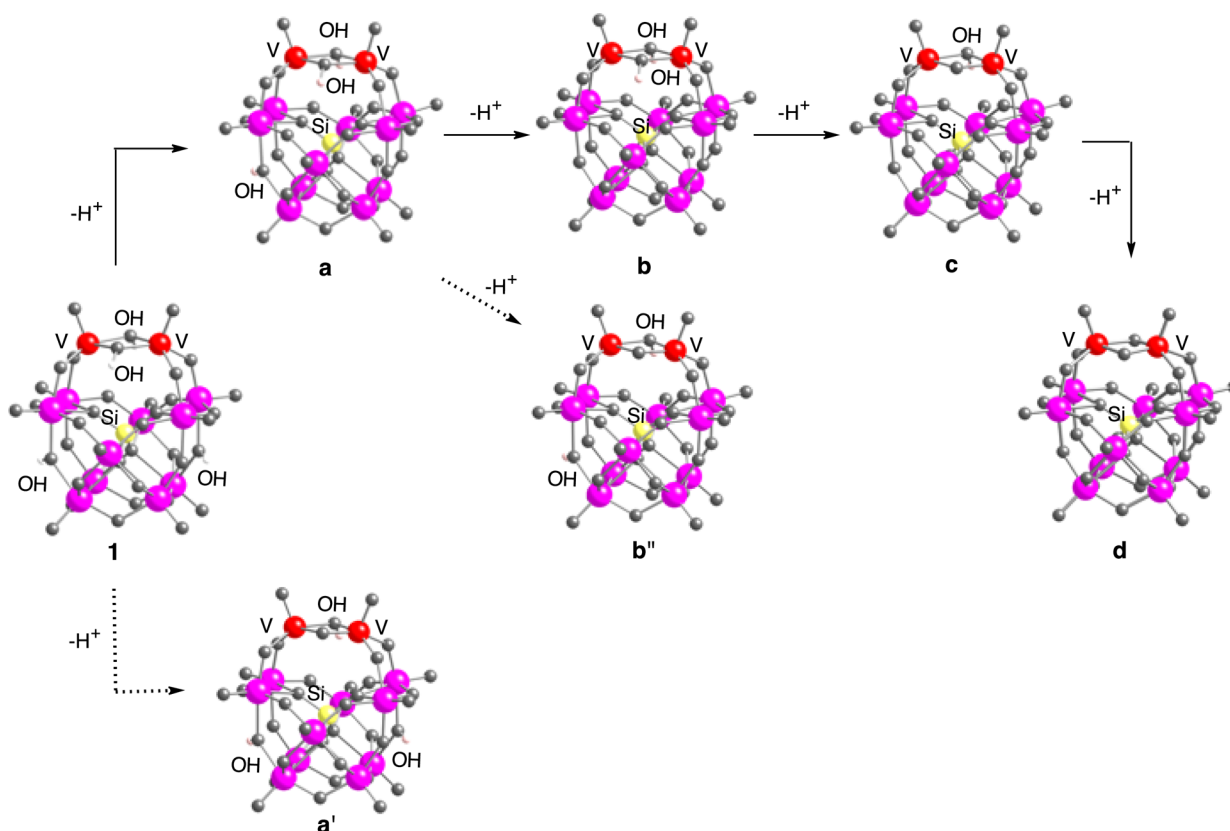


**Figure 2.** Deprotonation pathways from  $[\gamma-SiV_2W_{10}O_{36}(\mu-OH)_4]^{4+}$  (**1**) to  $[\gamma-SiV_2W_{10}O_{40}]^{8-}$  (**d**).

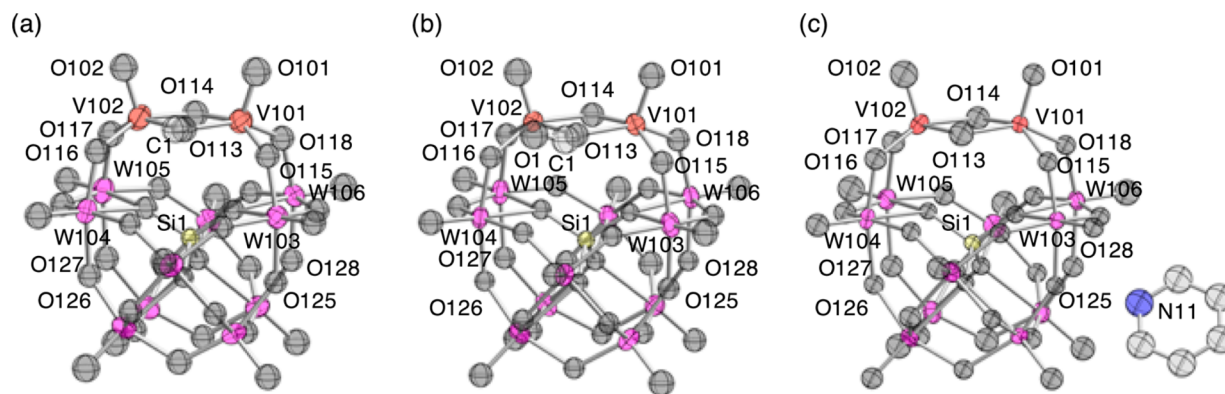


**Figure 3.** ORTEP views of (a)  $(\text{TBA})_4[\gamma\text{-SiV}^{\text{IV}}_2\text{W}_{10}\text{O}_{36}(\mu\text{-OH})_3(\mu\text{-OMe})]$  (**2·Me**), (b)  $(\text{TBA})_4[\gamma\text{-SiV}^{\text{IV}}_2\text{W}_{10}\text{O}_{36}(\mu\text{-OH})_3(\mu\text{-OCH(O)H})]$  (**3**), and (c)  $(\text{TBA})_4(\text{PyH})[\gamma\text{-SiV}^{\text{IV}}_2\text{W}_{10}\text{O}_{37}(\mu\text{-OH})_3]$  (**PyH·4**) drawn at the 50% probability level.

**Table 2.** Crystallographic Data for  $(\text{TBA})_4[\gamma\text{-SiV}^{\text{IV}}_2\text{W}_{10}\text{O}_{36}(\mu\text{-OH})_3(\mu\text{-OMe})]$  (**2·Me**),  $(\text{TBA})_4[\gamma\text{-SiV}^{\text{IV}}_2\text{W}_{10}\text{O}_{36}(\mu\text{-OH})_3(\mu\text{-OCH(O)H})]$  (**3**),  $(\text{TBA})_4(\text{PyH})[\gamma\text{-SiV}^{\text{IV}}_2\text{W}_{10}\text{O}_{37}(\mu\text{-OH})_3]$  (**PyH·4**), and  $(\text{TBA})_5[\gamma\text{-SiV}^{\text{IV}}_2\text{W}_{10}\text{O}_{37}(\mu\text{-OH})_3]$  (**TBA·4**)

	<b>2·Me</b>	<b>3</b>	<b>PyH·4</b>	<b>TBA·4</b>
empirical formula	$\text{C}_{65}\text{N}_4\text{O}_{40}\text{SiV}_2\text{W}_{10}$	$\text{C}_{65}\text{N}_4\text{O}_{41}\text{SiV}_2\text{W}_{10}$	$\text{C}_{69}\text{N}_5\text{O}_{40}\text{SiV}_2\text{W}_{10}$	$\text{C}_{160}\text{N}_{10}\text{O}_{80}\text{Si}_2\text{V}_4\text{W}_{20}$
formula wt	3445.16	3461.16	3572.57	3639.2582
cryst syst	orthorhombic	orthorhombic	orthorhombic	monoclinic
lattice type	primitive	primitive	primitive	primitive
space group	$P2_12_12_1$ (No. 19)	$P2_12_12_1$ (No. 19)	$P2_12_12_1$ (No. 19)	$P2_1$ (No. 4)
lattice params				
<i>a</i> , Å	14.85630(10)	14.83890(10)	14.5951(2)	29.5573(6)
<i>b</i> , Å	23.7771(2)	24.4643(2)	18.0490(4)	15.5841(3)
<i>c</i> , Å	31.1135(3)	31.1980(2)	39.4695(8)	29.7037(7)
<i>V</i> , Å <sup>3</sup>	10990.52(16)	11325.60(14)	10397.3(3)	12934.3(5)
<i>Z</i>	4	4	4	2
<i>d</i> <sub>calcd</sub> , g cm <sup>-3</sup>	2.082	2.147	2.241	1.876
<i>F</i> <sub>000</sub>	6152	6596	6276	6592
$\mu(\text{Mo K}\alpha)$ , mm <sup>-1</sup>	10.658	10.344	11.268	9.062
no. of rflns	16448	15555	30125	35475
no. of observns	14044	15047	10818	25079
no. of variables	314	335	316	624
<i>R</i> 1 <sup>a</sup>	0.0547	0.0445	0.0806	0.0874
w <i>R</i> 2 <sup>a</sup>	0.1435	0.1168	0.2117	0.1789

<sup>a</sup>Data with  $I > 2.00\sigma(I)$ .

**Table 3.** Selected Bond Distances (Å) and Angles (deg) for  $(\text{TBA})_4[\gamma\text{-SiV}^{\text{IV}}_2\text{W}_{10}\text{O}_{36}(\mu\text{-OH})_3(\mu\text{-OMe})]$  (**2·Me**),  $(\text{TBA})_4[\gamma\text{-SiV}^{\text{IV}}_2\text{W}_{10}\text{O}_{36}(\mu\text{-OH})_3(\mu\text{-OCH(O)H})]$  (**3**),  $(\text{TBA})_4(\text{PyH})[\gamma\text{-SiV}^{\text{IV}}_2\text{W}_{10}\text{O}_{37}(\mu\text{-OH})_3]$  (**PyH·4**), and  $(\text{TBA})_5[\gamma\text{-SiV}^{\text{IV}}_2\text{W}_{10}\text{O}_{37}(\mu\text{-OH})_3]$  (**TBA·4**)

	<b>2·Me</b>	<b>3</b>	<b>PyH·4</b>	<b>TBA·4<sup>b</sup></b>	
				molecule A	molecule B
V=O	1.591(16), 1.600(15)	1.599(13), 1.576(13)	1.59(2), 1.57(3)	1.61(2), 1.63(2)	1.55(3), 1.65(3)
V–O(–V)	1.953(14), 1.984(14)	2.010(11), 2.009(12)	1.99(3), 1.98(2)	1.97(2), 1.971(18)	1.97(2), 2.00(2)
	1.970(14), 1.925(15)	2.009(12), 1.991(11)	2.01(3), 1.98(2)	1.981(19), 1.974(18)	1.99(2), 1.96(2)
V–O(–W)	1.879(13), 1.893(14)	1.915(11), 1.910(10)	1.95(2), 1.95(2)	1.931(18), 1.93(2)	1.96(2), 1.95(2)
	1.930(14), 1.876(13)	1.905(11), 1.898(10)	1.86(2), 1.97(2)	1.920(18), 1.929(18)	1.96(2), 2.02(2)
V···O(–Si)	2.74(1), 2.77(2)	2.75(1), 2.74(1)	2.78(2), 2.66(2)	2.74(2), 2.71(2)	2.73(2), 2.77(2)
Si–O	1.601(11), 1.613(12)	1.620(9), 1.619(9)	1.60(2), 1.64(2)	1.638(15), 1.634(18)	1.644(17), 1.603(16)
	1.633(11), 1.626(11)	1.630(9), 1.644(9)	1.621(19), 1.619(19)	1.688(18), 1.639(16)	1.658(17), 1.632(16)
V···V	3.094(5)	3.146(4)	3.076(8)	3.125(6)	3.085(8)
V–O–V	104.1(7), 104.6(7)	103.0(5), 103.7(5)	100.4(11), 101.9(11)	104.5(9), 104.8(9)	102.4(11), 102.3(11)
torsion angle <sup>a</sup>	2.231	0.893	2.341	1.018	1.022

<sup>a</sup>O101–V101···V102–O102 angle. <sup>b</sup>Molecules A and B are crystallographically independent.

W (5.926–6.325), O (1.694–2.108), and Si (3.956) of **3** suggested that the respective valences of V, W, O, and Si in **2·**

**Me** and **3** are +4, +6, –2, and +4.<sup>15,16</sup> The V–O–V angles for **2·Me** (104.1(7) and 104.6(7)°) and **3** (103.0(5) and

103.7(5)°) were comparable to each other. On the other hand, the V...V distances for **2·Me** (3.094(5) Å) and **3** (3.146(4) Å) were slightly different from each other. The difference is probably due to the different electronic effects of the bridging ligand (i.e., electron-donating ligand vs electron-withdrawing ligand). The V<sup>IV</sup>...O(-Si) distances for **2·Me** were 2.74(1) and 2.77(2) Å, and those for **3** were 2.75(1) and 2.74(1) Å, respectively. These V<sup>IV</sup>...O(-Si) distances for **2·Me** and **3** were longer than those of **1** and the vanadium(V) derivative **A** (2.53(1)–2.58(1) Å).<sup>7c</sup> In **3**, the C1A–O1A and C1A–O113 distances were 1.21(12) and 1.24(5) Å, respectively, and the O1A–C1A–O113 angle was 134(7)°, suggesting the  $\pi$  conjugation of O1A–C1A–O113 orbitals in the formate ligand.<sup>17</sup> The  $\pi$ -conjugation of the carboxyl moiety was also found in SOMO2 of **3** (Figure S8 (Supporting Information)). There have been only a few examples of monodentate bridging formate complexes to date.<sup>18</sup>

**Acidic Properties of (TBA)<sub>4</sub>[ $\gamma$ -SiV<sup>IV</sup><sub>2</sub>W<sub>10</sub>O<sub>36</sub>( $\mu$ -OH)<sub>4</sub>] (1).** Compound **1** was dissolved in acetonitrile containing ca. 2.5 equiv of pyridine, and the successive addition of diethyl ether gave dark brown solids in a moderate yield (66%). Single-crystal X-ray crystallography revealed the formation of (TBA)<sub>4</sub>(PyH)[ $\gamma$ -SiV<sup>IV</sup><sub>2</sub>W<sub>10</sub>O<sub>37</sub>( $\mu$ -OH)<sub>3</sub>] (PyH·**4**), in which pyridinium interacted with the [ $\gamma$ -SiW<sub>10</sub>O<sub>36</sub>]<sup>8-</sup> framework via a hydrogen-bonding interaction (Figure 1a; N11...O(125) (O(128)) 2.81(6) Å (2.92(6) Å)). One of two hydroxides spanning tungsten atoms reacted with pyridine to form pyridinium.<sup>19</sup> The BVS values were V (4.094, 4.368), W (5.774–6.558), Si (4.046), and O (1.658–2.127), suggesting that the respective valences are +4, +6, +4, and –2. The BVS values for O(113), O(114), and O(126) were 1.146, 1.209, and 1.576, respectively, suggesting that all these valences are –1 and that the OH moieties are retained. The W(104)–O(126) distance (2.07(2) Å) was longer than the W(106)–O(128) distance (2.02(2) Å), which was comparable to unprotonated W(103)–O(125) and W(105)–O(127) distances (2.02(2) and 2.04(3) Å). The BVS value for O(128) was 1.903. All of these results show that the deprotonation takes place at O(128).

The V<sup>IV</sup>(101)...V<sup>IV</sup>(102) distance was 3.076(8) Å, shorter than that of **1** (3.101(5) Å). In addition, the V<sup>IV</sup>–O–V<sup>IV</sup> angles (100.4(11) and 101.9(11)°) were smaller than those of **1** (103.1(9) and 103.1(6)°). The V<sup>IV</sup>(101)...O(137) and V<sup>IV</sup>(102)...O(138) distances were 2.78(2) and 2.66(2) Å, respectively, longer than V<sup>V</sup>...O(-Si) distances of the vanadium(V) species (TBA)<sub>4</sub>[ $\gamma$ -SiV<sup>V</sup><sub>2</sub>W<sub>10</sub>O<sub>38</sub>( $\mu$ -OH)<sub>2</sub>] (2.511(11) and 2.531(11) Å). The phenomena are characteristic of the Jahn–Teller effect.

The acidic nature of the hydroxyl groups of **1** was also confirmed by the reaction of **1** with 1 equiv of aqueous TBAOH (10 wt %) in 1,2-dichloroethane. A dark brown solid was obtained by the addition of toluene as a poor solvent (34%). Cold-spray mass spectroscopy (CSI-MS) showed a signal centered at *m/z* 4065.46 (*m/z* 4066.18 calculated for {(TBA)<sub>6</sub>[SiV<sub>2</sub>W<sub>10</sub>O<sub>37</sub>(OH)<sub>3</sub>]}<sup>+</sup>), suggesting the formation of a monodeprotonated product from **1**. Single-crystal X-ray crystallography confirmed the formation of (TBA)<sub>5</sub>[ $\gamma$ -SiV<sup>IV</sup><sub>2</sub>W<sub>10</sub>O<sub>37</sub>( $\mu$ -OH)<sub>3</sub>] (TBA·**4**), where one of the protons between two tungsten atoms were deprotonated (Figure S6 in the Supporting Information).<sup>20</sup>

**Amphiprotic Properties of (TBA)<sub>4</sub>[ $\gamma$ -SiV<sup>IV</sup><sub>2</sub>W<sub>10</sub>O<sub>36</sub>( $\mu$ -OH)<sub>4</sub>] (1).** As described above, compound **1** exhibited amphiprotic behaviors and acted as both an acid and a base. Reduction of the vanadium centers from +5 to +4 produces

additional protons on the POM framework to form more acidic OH groups between tungsten atoms. To the best of our knowledge, few inorganic compounds with different kinds of hydroxide groups inside the same molecule have been reported to date. Since the pK<sub>a</sub> value for pyridine is 12.53,<sup>21</sup> pyridine effectively acts as a Lewis base to react with a proton (pK<sub>a</sub>(1) = 11.32) residing on the bridging oxo moiety between two tungsten atoms. Upon the addition of an excess amount of pyridine, additional pyridinium was not formed. This is because pK<sub>a</sub>(2) is calculated to be 17.78 from DFT calculations and is larger than that of pyridine. On the other hand, pK<sub>a</sub> values for MeOH and HCOOH are 15.5 and 3.75, respectively, and these molecules can act as acids toward hydroxides (pK<sub>a</sub>(2) = 16.46) between two vanadium atoms. Generally, the basic property in a polybasic acid such as H<sub>2</sub>CO<sub>3</sub> does not evolve without deprotonation. Therefore, it is noteworthy that the more basic hydroxide in **1** reacts with more acidic substrates without the deprotonation of acidic hydroxides.

## CONCLUSION

In summary, the amphiprotic properties of a bis( $\mu$ -hydroxo)-divanadium(IV)-substituted  $\gamma$ -Keggin-type silicodecatungstate, (TBA)<sub>4</sub>[ $\gamma$ -SiV<sup>IV</sup><sub>2</sub>W<sub>10</sub>O<sub>36</sub>( $\mu$ -OH)<sub>4</sub>] (**1**), with two different kinds of hydroxyl groups were investigated. The isoelectronic substitution of “V<sup>5+</sup>” in (TBA)<sub>4</sub>[ $\gamma$ -SiV<sup>V</sup><sub>2</sub>W<sub>10</sub>O<sub>38</sub>( $\mu$ -OH)<sub>2</sub>] with “V<sup>4+</sup> + H<sup>+</sup>” resulted in the formation of (TBA)<sub>4</sub>[ $\gamma$ -SiV<sup>IV</sup><sub>2</sub>W<sub>10</sub>O<sub>38</sub>( $\mu$ -OH)<sub>4</sub>] with more acidic protons at oxygen atoms between two tungsten atoms. Dehydrative condensation reactions of **1** with methanol and formic acid proceeded on more basic hydroxyl groups between two vanadium atoms without the deprotonation of more acidic hydroxides between two tungsten atoms to form (TBA)<sub>4</sub>[ $\gamma$ -SiV<sup>IV</sup><sub>2</sub>W<sub>10</sub>O<sub>36</sub>( $\mu$ -OH)<sub>3</sub>( $\mu$ -OR)] (**2·R**, R = Me, Et, Pr; **3**, R = C(O)H), showing Brønsted base properties of the hydroxyl groups between two vanadium atoms. On the other hand, the hydroxyl groups between tungsten atoms exhibited Brønsted acid properties and reacted with pyridine (Py) and TBAOH to form (TBA)<sub>4</sub>A[ $\gamma$ -SiV<sup>IV</sup><sub>2</sub>W<sub>10</sub>O<sub>37</sub>( $\mu$ -OH)<sub>3</sub>] (PyH·**4**, A = PyH; TBA·**4**, A = TBA). DFT calculations for [ $\gamma$ -SiV<sup>IV</sup><sub>2</sub>W<sub>10</sub>O<sub>36</sub>( $\mu$ -OH)<sub>4</sub>]<sup>4-</sup> in water also supported both the acidic and basic nature of hydroxyl groups in **1**.

## EXPERIMENTAL SECTION

**General Procedures.** Compound **1** was synthesized according to our previous report.<sup>7a</sup> The manipulations were carried out under argon except for the synthesis of **1**. Dehydrated solvents such as 1,2-dichloroethane, acetonitrile, and toluene and a 10 wt % aqueous solution of TBAOH were used as purchased. <sup>1</sup>H (500 MHz), <sup>13</sup>C{<sup>1</sup>H} (124.50 MHz), <sup>29</sup>Si{<sup>1</sup>H} (98.37 MHz), and <sup>51</sup>V{<sup>1</sup>H} (130.23 MHz) NMR spectra were recorded on a JEOL ECA-500 instrument.<sup>22</sup> Infrared spectra were recorded on a JASCO FT-IR 580 instrument. CSI-MS spectra were measured with a JEOL T100-CS instrument.

**Synthesis of (TBA)<sub>4</sub>[ $\gamma$ -SiV<sup>IV</sup><sub>2</sub>W<sub>10</sub>O<sub>36</sub>( $\mu$ -OH)<sub>3</sub>( $\mu$ -OMe)] (2·Me).** Compound **1** (0.0501 g, 0.0014 mmol) was dissolved in 1 mL of acetonitrile, followed by the addition of MeOH (0.1 mL; 2.4 mmol). *n*-Butyl methyl ether was layered onto the acetonitrile solution, and the resulting solution was allowed to stand overnight. The dark brown solid of (TBA)<sub>4</sub>[ $\gamma$ -SiV<sup>IV</sup><sub>2</sub>W<sub>10</sub>O<sub>36</sub>( $\mu$ -OH)<sub>3</sub>( $\mu$ -OMe)] (**2·Me**; 0.0276 g, 0.0077 mmol) was obtained in 54.9% yield. IR (KBr): 2961 m, 2932 m, 2873 m ( $\nu_{C-H}$ ), 1484 m, 1383 m, 1152 w, 1096 w, 1070 w, 1003 m, 976 m, 960 s, 915 vs, 898 s, 865 vs, 811 s, 774 s, 736 m, 701 m, 552 m, 510 w, 400 w, 387 m, 364 m, 352 m, 331 w, 310 m, 302 m, 286 m cm<sup>-1</sup>. CSI-MS (positive, MeCN): *m/z* 3839.36 (3838.63, TBA·**2·Me**<sup>+</sup>). Anal. Calcd for C<sub>65</sub>H<sub>150</sub>N<sub>4</sub>SiV<sub>2</sub>W<sub>10</sub>O<sub>40</sub>: C, 21.71; H, 4.20; N, 1.56. Found: C, 22.29; H, 4.36; N, 1.49. The ethoxo and propoxo

derivatives **2·Et** and **2·Pr** were obtained by similar procedures. Data for **2·Et** (0.0321 g, 0.0089 mmol, 63.3% yield) are as follows. IR (KBr): 2961 s, 2935 m, 2873 m ( $\nu_{C-H}$ ), 1483 m, 1380 m, 1152 w, 1095 m, 1042 m, 1000 m, 961 s, 916 vs, 902 vs, 869 vs, 797 vs, 779 vs, 737 s, 703 s, 553 m, 456 w, 388 m, 356 m, 330 m, 310 m, 300 m, 286 m  $\text{cm}^{-1}$ . CSI-MS (positive, MeCN):  $m/z$  3852.36 (3852.74, TBA·**2·Et**<sup>+</sup>). Anal. Calcd for  $\text{C}_{66}\text{H}_{152}\text{N}_4\text{SiV}_2\text{W}_{10}\text{O}_{40}$ : C, 21.96; H, 4.24; N, 1.55. Found: C, 21.96; H, 4.24; N, 1.55. Data for **2·Pr** are as follows (0.0418 g, 0.00115 mmol, 82.0% yield). IR (KBr): 2961 m, 2934 m, 2873 m ( $\nu_{C-H}$ ), 1483 m, 1381 m, 1151 w, 1106 w, 992 m, 963 s, 918 vs, 903 vs, 871 vs, 791 vs, 702 m, 554 m, 458 w, 407 m, 389 m, 356 m, 332 w, 310 w, 302 w, 287 w, 277 w  $\text{cm}^{-1}$ . CSI-MS (positive, MeCN):  $m/z$  3866.42 (3866.67, TBA·**2·Pr**<sup>+</sup>). Anal. Calcd for  $\text{C}_{67}\text{H}_{154}\text{N}_4\text{SiV}_2\text{W}_{10}\text{O}_{40}$ : C, 22.20; H, 4.28; N, 1.55. Found: C, 21.95; H, 4.35; N, 1.49.

**Synthesis of (TBA)<sub>4</sub>[ $\gamma$ -SiV<sup>IV</sup>W<sub>10</sub>O<sub>36</sub>( $\mu$ -OH)<sub>3</sub>( $\mu$ -OCH(O)H)] (3).** Compound **1** (0.0498 g, 0.014 mmol) was dissolved in 2 mL of 1,2-dichloroethane, followed by the addition of formic acid (10  $\mu\text{L}$ ; 0.27 mmol). Diethyl ether (1 mL) was layered onto the 1,2-dichloroethane solution, and the resulting solution was allowed to stand overnight. The dark brown solid of (TBA)<sub>4</sub>[ $\gamma$ -SiV<sup>IV</sup>W<sub>10</sub>O<sub>36</sub>( $\mu$ -OH)<sub>3</sub>( $\mu$ -OCH(O)H)] (**3**; 0.0287 g, 0.0074 mmol) was obtained in 61.2% yield. IR (KBr): 2961 m, 2935 m, 2873 m, 1671 m ( $\nu_{\text{CO}}$ ), 1483 m, 1382 m, 1217 w, 1152 w, 1107 w, 1063 w, 1006 m, 976 m, 963 s, 909 vs, 866 s, 800 s, 766 s, 716 s, 551 m, 389 m, 359 m, 319 w, 303 w, 291 w, 283 w, 268 w  $\text{cm}^{-1}$ . CSI-MS (positive, MeCN):  $m/z$  3852.59 (3852.62, TBA·**3**<sup>+</sup>). Anal. Calcd for  $\text{C}_{65}\text{H}_{148}\text{N}_4\text{SiV}_2\text{W}_{10}\text{O}_{41}$ : C, 21.62; H, 4.13; N, 1.55. Found: C, 21.44; H, 4.23; N, 1.29.

**Synthesis of (TBA)<sub>4</sub>(PyH)[ $\gamma$ -SiV<sup>IV</sup>W<sub>10</sub>O<sub>37</sub>( $\mu$ -OH)<sub>3</sub>] (PyH·4).** Compound **1** (0.0498 g, 0.014 mmol) was dissolved in 1 mL of acetonitrile, followed by the addition of pyridine (3  $\mu\text{L}$ ; 0.037 mmol). Diethyl ether (3 mL) was layered onto the acetonitrile solution, and the resulting solution was allowed to stand overnight. The dark brown solid of (TBA)<sub>4</sub>(PyH)[ $\gamma$ -SiV<sup>IV</sup>W<sub>10</sub>O<sub>37</sub>( $\mu$ -OH)<sub>3</sub>] (PyH·**4**; 0.0338 g, 0.0092 mmol) was obtained in 66.4% yield. IR (KBr): 3483 w ( $\nu_{\text{O-H}}$ ), 3131 w, 3065 w ( $\nu_{C-H}$ ), 2961 m, 2934 m, 2873 m ( $\nu_{C-H}$ ), 1535 w (PyH), 1484 m, 1382 m, 1152 w, 1106 w, 994 m, 965 s, 904 vs, 871 vs, 838 m, 789 vs, 694 m, 604 w, 548 m, 482 w, 455 w, 405 m, 389 m, 366 w, 355 m, 330 m, 310 w, 302 w, 292 w, 281 m  $\text{cm}^{-1}$ . The CSI-MS spectrum of **2** could not be detected due to instability in solution. Anal. Calcd for  $\text{C}_{69}\text{H}_{153}\text{N}_5\text{SiV}_2\text{W}_{10}\text{O}_{40}$ : C, 22.64; H, 4.21; N, 1.91. Found: C, 22.08; H, 4.19; N, 1.77.

**Synthesis of (TBA)<sub>5</sub>[ $\gamma$ -SiV<sup>IV</sup>W<sub>10</sub>O<sub>37</sub>( $\mu$ -OH)<sub>3</sub>] (TBA·4).** Compound **1** (0.0500 g, 0.0014 mmol) was dissolved in 1 mL of 1,2-dichloroethane, followed by the addition of 1 equiv of TBAOH (10 wt %). The addition of toluene onto the solution gave dark brown crystals of (TBA)<sub>5</sub>[ $\gamma$ -SiV<sup>IV</sup>W<sub>10</sub>O<sub>37</sub>( $\mu$ -OH)<sub>3</sub>] (TBA·**4**; 0.017 g, 0.476  $\mu\text{mol}$ , 34% yield). IR (KBr): 3670 w, 3491 w ( $\nu_{\text{O-H}}$ ), 2961 s, 2934 s, 2872 s, 1634 m, 1484 s, 1381 m, 1281 w, 1152 w, 1107 w, 1057 w, 1027 w, 997 m, 984 m, 966 s, 952 s, 907 vs, 892 vs, 863 vs, 820 s, 791 s, 698 s, 551 m, 475 w, 459 w, 396 m, 389 m, 377 m, 355 m, 311 m, 291 w, 283 w, 277 w  $\text{cm}^{-1}$ . CSI-MS (positive, MeCN):  $m/z$  4065.46 ( $m/z$  4066.18 calculated for  $\{(\text{TBA})_6[\text{SiV}_2\text{W}_{10}\text{O}_{37}(\text{OH})_3]\}^+$ ). Anal. Calcd for  $\text{C}_{80}\text{H}_{180}\text{N}_5\text{SiV}_2\text{W}_{10}\text{O}_{40}$ : C, 25.13; H, 4.82; N, 1.83. Found: C, 25.40; H, 4.55; N, 1.77.

**X-ray Crystallography.** Diffraction measurements were made on a Rigaku MicroMax-007 instrument with Mo K $\alpha$  radiation ( $\lambda = 0.71069 \text{ \AA}$ ). The data collections were carried out at 153 K. Indexing was performed from 12 oscillation images, which were exposed for 5 s. The crystal to detector distance was 45 mm. Readout was performed with a pixel size of 72.4  $\times$  72.4 mm. A sweep of data was done using  $\omega$  scans from  $-110$  to  $70^\circ$  at  $\kappa = 45^\circ$  and  $\phi = 0, 90^\circ$ . A total of 720 images for each compound was collected. Neutral scattering factors were obtained from the standard source.<sup>23</sup> Data were corrected for Lorentz and polarization effects. Empirical absorption corrections were made with HKL 2000 for Linux.<sup>24</sup> Molecular structures were solved by SHELX-97<sup>25</sup> linked to Win-GX for Windows.<sup>26</sup> For **2·Me**, **3**, and TBA·**4** the SQUEEZE program of PLATON was used to remove the electron density on the Fourier map derived from the disordered

solvents of crystallization.<sup>27</sup> More detailed information on X-ray crystallography is provided in the Supporting Information.

## ■ ASSOCIATED CONTENT

### 📄 Supporting Information

Text, tables, figures, and CIF files giving crystallographic data of **2·Me**, **2·Et**, **2·Pr**, **3**, PyH·**4**, and TBA·**4**, experimental procedures, details of X-ray crystallography, and details of DFT calculations. This material is available free of charge via the Internet at <http://pubs.acs.org>. CCDC file numbers 988984 (**2·Me**), 988985 (**2·Et**), 988986 (**2·Pr**), 988987 (**3**), 988988 (PyH·**4**), and 988989 (TBA·**4**) also contain supplementary crystallographic data. The data can be obtained free of charge via [www.ccdc.cam.ac.uk/conts/retrieving.html](http://www.ccdc.cam.ac.uk/conts/retrieving.html) (or from the Cambridge Crystallographic Data Centre, 12, Union Road, Cambridge CB2 1EZ, U.K.; fax (+44) 1223-336-033; e-mail deposit@ccdc.cam.ac.uk).

## ■ AUTHOR INFORMATION

### ✉ Corresponding Author

\*N.M.: e-mail, [tmizuno@mail.ecc.u-tokyo.ac.jp](mailto:tmizuno@mail.ecc.u-tokyo.ac.jp); tel, +81-3-5841-7272; fax, +81-3-5841-7220.

### 📝 Notes

The authors declare no competing financial interest.

## ■ ACKNOWLEDGMENTS

This work was supported by Grants-in-Aid for Scientific Research, Ministry of Education, Culture, Science, Sports and Technology of Japan (MEXT), and the Funding Program for World-Leading Innovative R&D on Science and Technology (FIRST Program) of the Japan Society for the Promotion of Science (JSPS).

## ■ REFERENCES

- (1) (a) Atkins, P.; Overton, T.; Rourke, J.; Weller, M.; Armstrong, A., In *Shriver & Atkins Inorganic Chemistry*, Fourth ed., Oxford University Press, 2006. (b) Brönsted, J. N. *Recl. Trav. Chim. Pays-Bas* **1923**, *42*, 718–728. (c) Lowry, T. M. *Trans. Faraday Soc.* **1924**, *20*, 13–15. (d) Brönsted, J. N. *J. Phys. Chem.* **1926**, *30*, 777–790.
- (2) (a) Roesky, H. W.; Murugavel, R.; Walawalkar, M. G. *Chem. Eur. J.* **2004**, *10*, 324–331. (b) Gijje, J. W.; Roesky, H. W. *Chem. Rev.* **1994**, *94*, 895–910.
- (3) (a) Abboud, J.-L. M.; Sraidi, K.; Abraham, M. H.; Taft, R. W. *J. Org. Chem.* **1990**, *55*, 2230–2232. (b) Abboud, J.-L. M.; Roussel, C.; Gentric, E.; Sraidi, K.; Lauransan, J.; Guihéneuf, G.; Kamlet, M. J.; Taft, R. W. *J. Org. Chem.* **1988**, *53*, 1545–1550. (c) Abboud, J.-L. M.; Sraidi, K.; Guihéneuf, G.; Negro, A.; Kamlet, M. J.; Taft, R. W. *J. Org. Chem.* **1985**, *50*, 2870–2873. (d) Sisler, H. H.; Davidson, A. W.; Stoenner, R.; Lyon, L. L. *J. Am. Chem. Soc.* **1944**, *66*, 1888–1892.
- (4) (a) Roesky, H. W.; Singh, S.; Yusuff, K. K. M.; Maguire, J. A.; Hosmane, N. S. *Chem. Rev.* **2006**, *106*, 3813–3843. (b) Cradwick, C. P. G.; Farmer, V. C.; Russell, J. D.; Masson, C. R.; Wada, K.; Yoshinaga, N. *Nature* **1972**, *240*, 187–189.
- (5) (a) Thematic issue on polyoxometalate: *Chem. Rev.* **1998**, *98*, 1. (b) *Polyoxometalate Chemistry for Nano-Composite Design*; Yamase, T., Pope, M. T., Eds.; Kluwer: Dordrecht, The Netherlands, 2002. (c) Kozhevnikov, I. V. In *Catalysis by Polyoxometalates*; Wiley: Chichester, U.K., 2002. (d) Pope, M. T. In *Comprehensive Coordination Chemistry II*; Wedd, A. G., McCleverty, J. A., Meyer, T. J., Eds.; Elsevier: New York, 2004; Vol. 4, p 635. (e) Hill, C. L. In *Comprehensive Coordination Chemistry II*; Wedd, A. G., McCleverty, J. A., Meyer, T. J., Eds.; Elsevier: New York, 2004; Vol. 4, p 679. (f) Neumann, R. In *Modern Oxidation Methods*; Bäckvall, J. E., Ed.; Wiley-VCH: Weinheim, Germany, 2004; p 223. (g) Bassil, B. S.; Kortz, U. *J. Chem. Soc., Dalton Trans.* **2011**, *40*, 9649–9661.

(6) (a) Besson, C.; Musaev, D. G.; Lahootun, V.; Cao, R.; Chamoreau, L.-M.; Villanneau, R.; Villain, F.; Thouvenot, R.; Geletii, Y. V.; Hill, C. L.; Proust, A. *Chem. Eur. J.* **2009**, *15*, 10233–10243. (b) Knoth, W. H.; Harlow, R. L. *J. Am. Chem. Soc.* **1981**, *103*, 4265–4266.

(7) (a) Uehara, K.; Fukaya, K.; Mizuno, N. *Angew. Chem., Int. Ed.* **2012**, *51*, 7715–7718. (b) Nakagawa, Y.; Uehara, K.; Mizuno, N. *Inorg. Chem.* **2005**, *44*, 9068–9075. (c) Nakagawa, Y.; Uehara, K.; Mizuno, N. *Inorg. Chem.* **2005**, *44*, 14–16. (d) Goto, Y.; Kamata, K.; Yamaguchi, K.; Uehara, K.; Hikichi, S.; Mizuno, N. *Inorg. Chem.* **2006**, *45*, 2347–2356. (e) Uehara, K.; Miyachi, T.; Nakajima, T.; Mizuno, N. *Inorg. Chem.* **2014**, *53*, 3907–3918.

(8) Frisch, M. J.; Trucks, G. W.; Schlegel, H. B.; Scuseria, G. E.; Robb, M. A.; Cheeseman, J. R.; Scalmani, G.; Barone, V.; Mennucci, B.; Petersson, G. A.; Nakatsuji, H.; Caricato, M.; Li, X.; Hratchian, H. P.; Izmaylov, A. F.; Bloino, J.; Zheng, G.; Sonnenberg, J. L.; Hada, K.; Ehara, M.; Toyota, K.; Fukuda, R.; Hasegawa, J.; Ishida, M.; Nakajima, T.; Honda, Y.; Kitao, O.; Nakai, H.; Vreven, T.; Montgomery, J. A., Jr.; Peralta, J. E.; Ogliaro, F.; Bearpark, M.; Heyd, J. J.; Brothers, E.; Kudin, K. N.; Staroverov, V. N.; Kobayashi, R.; Normand, J.; Raghavachari, K.; Rendell, A.; Burant, J. C.; Iyengar, S. S.; Tomasi, J.; Cossi, M.; Rega, N.; Millam, J. M.; Klene, M.; Knox, J. E.; Cross, J. B.; Bakken, V.; Adamo, C.; Jaramillo, J.; Gomperts, R.; Stratmann, R. E.; Yazyev, O.; Austin, A. J.; Cammi, R.; Pomelli, C.; Ochterski, J. W.; Martin, R. L.; Morokuma, K.; Zakrzewski, V. G.; Voth, G. A.; Salvador, P.; Dannenberg, J. J.; Dapprich, S.; Daniels, A. D.; Farkas, Ö.; Foresman, J. B.; Ortiz, J. V.; Cioslowski, J.; Fox, D. J. *Gaussian 09, Revision B.01*; Gaussian, Inc., Wallingford, CT, 2009.

(9) Tomasi, J.; Mennucci, B.; Cammi, R. *Chem. Rev.* **2005**, *105*, 2999–3094.

(10) Molekel 5.4 (the molecular visualization program developed by the visualization group at the Swiss national supercomputing center (CSCS)).

(11) Ho, J.; Coote, M. L. *Theor. Chem. Acc.* **2010**, *125*, 3–21.

(12) The space group  $P2_12_12_1$  is appropriate from the extinction rule. The Flack parameters of ca. 0.5 in **2·Me** and **3** suggest the disorder of the methoxo and formate bridging ligands.

(13) Since the formate moiety in **3** was disordered, the most probable  $sp^2$  C=O moiety was depicted.

(14) BVS calculations for **2·Et** and **2·Pr** are provided in Tables S4 and S5 in the Supporting Information.

(15) Brese, N. E.; O’Keeffe, M. *Acta Crystallogr., Sect. B* **1991**, *B47*, 192–197.

(16) The CSI-MS spectrum for **2·Et** contains  $m/z$  ca. 0.6 error probably because of instrument conditions such as the lens voltage. The CSI-MS spectra for **2·Me**, **2·Pr**, and **3** showed the corresponding ester derivatives with the retention of protons between two tungsten atoms. BVS values for vanadium atoms for **2·Et** were 4.191 and 4.162, suggesting that the valences of the vanadium atoms are +4. In addition, the  $V\cdots O(-Si)$  distances (2.73(3) and 2.80(2) Å) for **2·Et** are longer than those of the vanadium(V) derivative  $(TBA)_4[\gamma-SiV_2W_{10}O_{38}(\mu-OH)(\mu-OEt)]$  (2.56(2) and 2.53(2) Å<sup>7c</sup>), suggesting the Jahn–Teller effect characteristic of the vanadium(IV) species. All of these considerations suggest that the mixed-valence species is not formed.

(17) The delocalization of the bridging formate ligand was supported by the observation of the C=O stretching IR band at 1671  $cm^{-1}$ , which is lower than that of formic acid at 1727 (1722)  $cm^{-1}$ .

(18) (a) Escriva, E.; Server-Carrio, J.; Lezama, L.; Folgado, J.-V.; Pizarro, J. L.; Ballesteros, R.; Abarca, B. *J. Chem. Soc., Dalton Trans.* **1997**, 2033–2038. (b) Ni, J.; Qiu, Y.; Cox, T. M.; Jones, C. A.; Berry, C.; Melon, L. *Organometallics* **1996**, *15*, 4669–4671.

(19) The formation of pyridinium was also supported by the observation of an IR band at 1535  $cm^{-1}$ . (a) Pichon, C.; Mialane, P.; Marrot, J.; Binet, C.; Vimont, A.; Travert, A.; Lavalley, J.-C. *Phys. Chem. Chem. Phys.* **2011**, *13*, 322–327. (b) Topsøe, N.-Y.; Topsøe, H. *J. Catal.* **1989**, *119*, 252–255.

(20) The formation of  $(TBA)_4[\gamma-SiV_2W_{10}O_{36}(\mu-OH)_2(PhNHCO)_2]$  containing N-protonated phenyl isocyanate cations by reaction of **1**

with phenyl isocyanate was also supported by the acidic nature of OH moieties between two tungsten atoms.

(21) Kaljurand, I.; Kütt, A.; Sooväli, L.; Rodima, T.; Mäemets, V.; Leito, I.; Koppel, I. A. *J. Org. Chem.* **2005**, *70*, 1019–1028 and references cited therein.

(22) <sup>51</sup>V and <sup>29</sup>Si NMR signals derived from anionic parts could not be observed due to the paramagnetic effect. No <sup>1</sup>H NMR signals derived from OH moieties could be observed.

(23) *International Tables for X-ray Crystallography*; Kynoch Press: Birmingham, U.K., 1975; Vol. 4.

(24) Otwinowski, Z.; Minor, W. *Processing of X-ray Diffraction Data Collected in Oscillation Mode. Macromolecular Crystallography, Part A*; Carter, C. W., Jr., Sweet, R. M., Eds.; Academic Press: New York, 1997; *Methods in Enzymology* **276**, p 307.

(25) Sheldrick, G. M. *SHELX-97, Programs for Crystal Structure Analysis, release 97-2*; University of Göttingen, Göttingen, Germany, 1997.

(26) Farrugia, L. J. *J. Appl. Crystallogr.* **1999**, *32*, 837–838.

(27) Spek, A. L. *J. Appl. Crystallogr.* **2003**, *33*, 7–13.